ELSEVIER

Journal of Alloys and Compounds 452 (2008) 195–199

Journal of ALLOYS AND COMPOUNDS

www.elsevier.com/locate/jallcom

Bi doping effects on the physical properties of $Pr_{0.6}Sr_{0.4}Mn_{1-x}Bi_xO_3$ ($0 \leq x \leq 0.2$) manganese oxides

I. Kammoun [a], W. Cheikhrouhou-Koubaa [a], W. Boujelben [a], A. Cheikhrouhou [a,b,*]

[a] *Laboratoire de Physique des Matériaux, Faculté des Sciences de Sfax, B.P. 802, 3018 Sfax, Tunisia*
[b] *Laboratoire de Magnétisme Louis NEEL, B.P. 166, F-38042 Grenoble Cedex 9, France*

Received 10 October 2006; received in revised form 27 October 2006; accepted 1 November 2006
Available online 12 December 2006

Abstract

Structural, magnetic and magneto-caloric properties of $Pr_{0.6}Sr_{0.4}Mn_{1-x}Bi_xO_3$ ($0.0 \leq x \leq 0.2$) powder samples have been investigated. X-ray powder diffraction showed that all our synthesized samples are single phase and crystallize in the orthorhombic symmetry with *Pbnm* space group. The unit cell volume increases with increasing Bi content. Bi doping leads to a weakening of the ferromagnetic (FM) ordering at low temperature, the Curie temperature T_c decreases from 310 K for $x = 0.0$ to 225 K for $x = 0.2$. The critical exponent γ deduced from the $M(H)$ curves is found to be $\gamma = 0.33$ for $Pr_{0.6}Sr_{0.4}Mn_{0.9}Bi_{0.1}O_3$ sample. A large magneto-caloric effect has been detected with a maximum of magneto-entropy change, $|\Delta S_{max}|$, of 0.95 and 2 J/kg K at 1 and 8 T, respectively, at 255 K for a Bi doping amount of 0.1.

PACS: 71.30.+h; 75.50.−y; 75.75

Keywords: Manganites; Curie temperature; Ferromagnetism; Magneto-caloric effect

1. Introduction

The perovskite-type manganese oxides $Ln_{1-x}A_xMnO_3$ (Ln is a trivalent rare-earth element and A is a divalent alkaline-earth or a monovalent alkali metal) have known a very big interest since the discovery of colossal magnetoresistance effects in such materials [1–6]. The substitution of the trivalent rare-earth element by a divalent or a monovalent one induces a mixed valence Mn^{3+} and Mn^{4+} ions. Substitutions in these materials lead to different crystal structures, spin states and transport properties. Magnetic and magneto-transport properties in perovskite manganese oxides were traditionally explained using the double exchange interaction which considers the exchange of electrons between neighbouring Mn^{3+} and Mn^{4+} sites with strong on-site Hund's coupling [7]. However, Millis et al. [8] suggested that other parameters also play a crucial role, such as charge ordering, average ionic radius $\langle r_A \rangle$ of the A-cation site [9], A-site cationic size mismatch [10], oxygen deficiency [11] and polaron effect due to the strong electron–phonon coupling arising from Jahn–Teller distortions [8]. These systems have been given much attention because they could possibly be used for sensor applications [12]. Several studies have been performed on the effects of the substitution in the A site [4,6,13,14], however only few studies have been reported on the substitution effects in the B site [15–18].

In this work, we elaborated $Pr_{0.6}Sr_{0.4}Mn_{1-x}Bi_xO_3$ ($0.0 \leq x \leq 0.2$) powder samples and studied the effects on the physical properties of the bismuth substitution in these materials.

2. Experimental

Powder samples $Pr_{0.6}Sr_{0.4}Mn_{1-x}Bi_xO_3$ ($0.0 \leq x \leq 0.2$) have been elaborated using the solid state reaction at high temperature by mixing Pr_6O_{11}, Bi_2O_3, $SrCO_3$ and MnO_2 up to 99.9% purity in the desired proportion according the following reaction:

$$0.1Pr_6O_{11} + (x/2)Bi_2O_3 + 0.4SrCO_3 + (1-x)MnO_2 \rightarrow Pr_{0.6}Sr_{0.4}Mn_{1-x}Bi_xO_3 + \delta CO_2$$

The starting materials were intimately mixed in an agate mortar and then heated in air at 1000 °C for 3 days with intermediate regrinding. After

* Corresponding author at: Laboratoire de Physique des Matériaux, Faculté des Sciences de Sfax, B.P. 802, 3018 Sfax, Tunisia. Tel.: +216 74 676607; fax: +216 74 676607.
E-mail address: abdcheikhrouhou@yahoo.fr (A. Cheikhrouhou).

0925-8388/$ – see front matter © 2006 Elsevier B.V. All rights reserved.
doi:10.1016/j.jallcom.2006.11.069

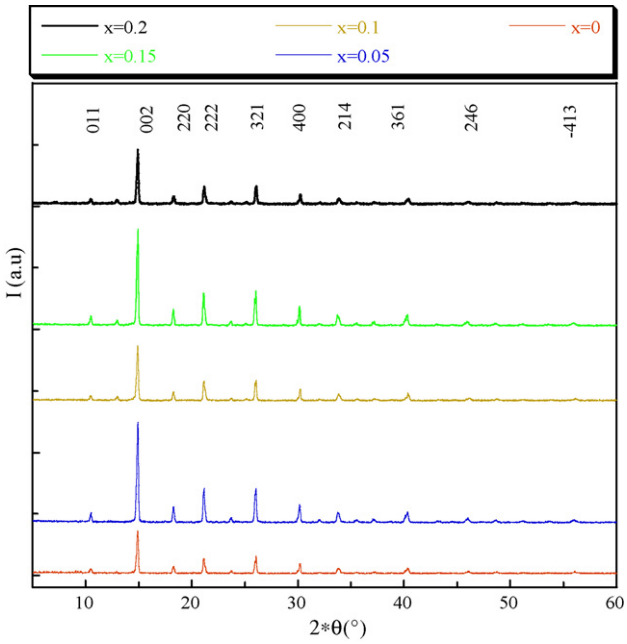

Fig. 1. X-ray diffraction patterns for $Pr_{0.6}Sr_{0.4}Mn_{1-x}Bi_xO_3$ samples.

pulverizing, the powders were pressed into pellets (of about 1 mm thickness) and sintered at 1400 °C in air for 3 days with intermediate regrinding and repelling. Finally, the pellets were rapidly quenched to room temperature in air. This step is done in order to retain the structure adopted at a given annealing temperature.

Phase purity, homogeneity, and cell dimensions are determined by powder X-ray diffraction at room temperature (diffractometer using Cu Kα radiation). Structural analysis has been carried out using the standard Rietveld technique [19].

Magnetization measurements versus temperature were recorded using a vibrating sample magnetometer in the temperature range 10–340 K, in an applied field of 500 Oe. The magnetization measurements versus magnetic applied field up to 8 T at several temperatures were recorded using an extraction magnetometer.

3. Results and discussion

3.1. X-ray diffraction analysis

X-ray diffraction analysis indicates that all our synthesized samples $Pr_{0.6}Sr_{0.4}Mn_{1-x}Bi_xO_3$ ($0.0 \le x \le 0.2$) are single phase without any detectable impurity. We plot in Fig. 1 the X-ray diffraction patterns for all our samples. All the reflection lines were successfully indexed according to an orthorhombic perovskite structure with *Pbnm* space group. By Bi doping no apparent structural changes can be identified. We list in Table 1 the unit cell volume and the lattice parameters for all

Table 1
Crystallographic data for $Pr_{0.6}Sr_{0.4}Mn_{1-x}Bi_xO_3$ samples

x	a (Å)	b (Å)	c (Å)	v (Å^3)
0.00	5.4500(0)	5.4803(6)	7.6926(4)	229.76
0.05	5.4500(1)	5.4843(6)	7.6922(4)	229.92
0.10	5.4500(6)	5.4889(8)	7.6917(4)	230.10
0.15	5.4501(1)	5.4936(9)	7.6912(4)	230.29
0.20	5.4501(6)	5.4983(9)	7.6907(3)	230.47

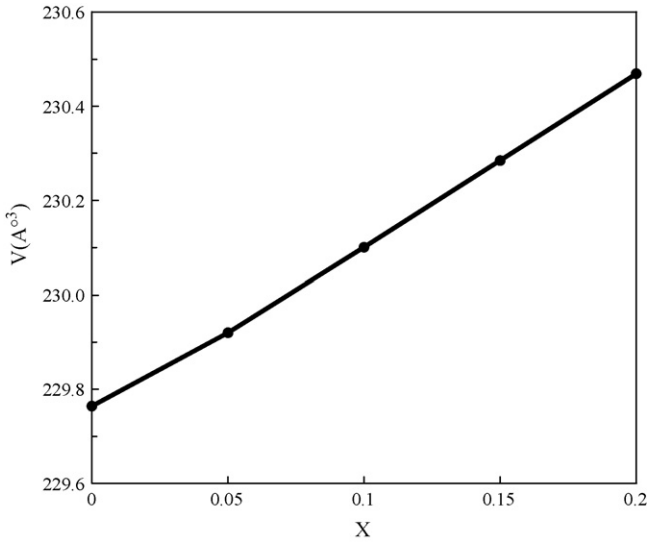

Fig. 2. Unit cell volume V as a function of x for $Pr_{0.6}Sr_{0.4}Mn_{1-x}Bi_xO_3$ samples.

our synthesized samples. While the a parameter remains constant, the b parameter increases and the c parameter decreases with increasing Bi content. The unit cell volume increases from 229.76 Å^3 for $x = 0$ to 230.47 Å^3 for $x = 0.2$ (Fig. 2) which can be explained by the increase of the Bi^{3+} content; in fact the Bi^{3+} ionic radius (1.03 Å) is larger than Mn^{3+} (0.58 Å) one. Rietveld refinement of the X-ray data of $Pr_{0.6}Sr_{0.4}Mn_{0.95}Bi_{0.05}O_3$ and

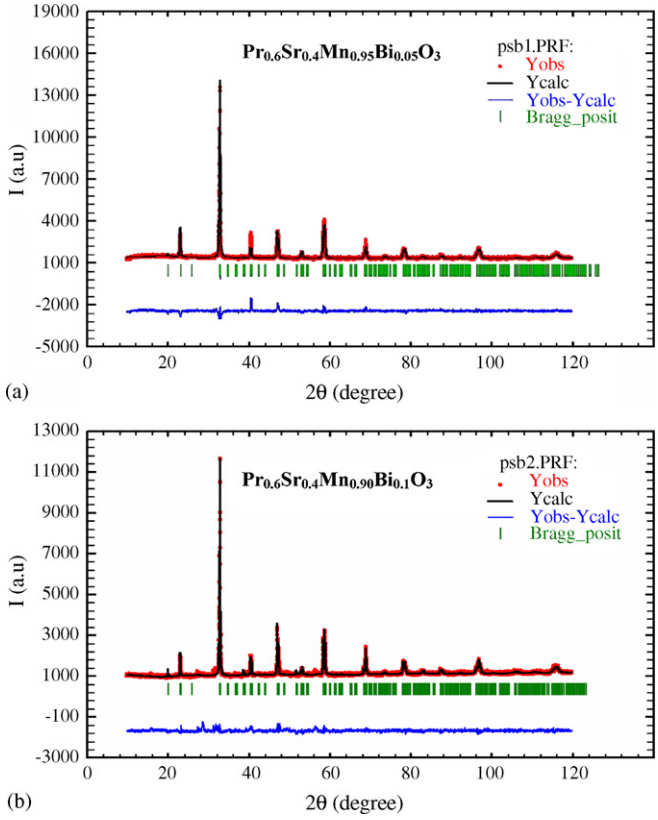

Fig. 3. (a) The 300 K powder X-ray diffraction pattern and refinement of $Pr_{0.6}Sr_{0.4}Mn_{0.95}Bi_{0.05}O_3$. (b) The 300 K powder X-ray diffraction pattern and refinement of $Pr_{0.6}Sr_{0.4}Mn_{0.9}Bi_{0.1}O_3$.

Table 2
Crystallographic data for $Pr_{0.6}Sr_{0.4}Mn_{0.95}Bi_{0.05}O_3$ and $Pr_{0.6}Sr_{0.4}Mn_{0.9}Bi_{0.1}O_3$ samples

Samples	$x=0.05$ (space group *Pbnm*)	$x=0.1$ (space group *Pbnm*)
Pr/Sr		
x	0.50050	0.48471
y	0.02395	−0.01096
z	0.25000	0.25000
Biso (Å^2)	1.19136	0.03653
Mn/Bi		
x	0.00000	0.00000
y	0.00000	0.00000
z	0.00000	0.00000
Biso (Å^2)	0.14932	−0.23017
O1		
x	0.77322	0.76594
y	0.23981	0.22491
z	0.25000	0.25000
Biso (Å^2)	−3.42606	−1.78113
O2		
x	1.31947	−3.09872
y	0.28994	9.19561
z	0.67708	4.36516
Biso (Å^2)	−3.42606	−1.78113
Residues of refinement		
R_p (%)	3.17	3.19
R_{wp} (%)	5.36	4.86
R_{exp} (%)	2.61	2.92
χ^2	2.237	2.76

$Pr_{0.6}Sr_{0.4}Mn_{0.9}Bi_{0.1}O_3$, was carried out using the FULLPROF code [19]. This program permits refinements on multiple samples. We plot in Fig. 3a and b the X-ray diffraction patterns at 300 K, including the observed and calculated profiles as well as the difference profile, for both samples. The quality of the refinement is evaluated through the goodness of fit indicator χ^2. Detailed results of the structural refinement are listed in Table 2.

3.2. Magnetic properties

The $Pr_{0.6}Sr_{0.4}MnO_3$ sample with 40% on Mn^{4+} is ferromagnetic below 310 K [13]. The $M(T)$ curve showed a sharp transition from paramagnetic to ferromagnetic sate followed by a decrease of the magnetization below 100 K which has been attributed to the coexistence, at low temperature, of two phases: an orthorhombic phase with *Pnma* space group (27%) and a monoclinic one with *I2/a* space group (73%). Moreover, the Mn moments ($3.47\mu_B$) lie antiparallel to the Pr ones ($0.11\mu_B$) in the component with *Pnma* symmetry while the Mn moments ($3.26\mu_B$) lie parallel to the Pr ones ($0.53\mu_B$) in the component with *I2/a* symmetry. In order to study the effect of the Bi doping upon the magnetic properties, we have performed magnetization measurements versus temperature under a magnetic applied field of 500 Oe. We plot in Fig. 4 the magnetization evolution versus temperature for $Pr_{0.6}Sr_{0.4}Mn_{1-x}Bi_xO_3$, all our samples exhibit a paramagnetic to ferromagnetic transition with decreasing temperature. The magnetization drop observed below 100 K in the parent compound disappears. The magnitude of the magnetization at low temperature decreases with increasing bismuth content. The Bi doping induces a weakening of the ferromagnetism at low temperatures in our samples. The Curie temperature T_c decreases from 310 K for $x=0.0$ to 225 K for $x=0.2$ (Fig. 5). As the bismuth ions enters into the samples as Bi^{3+} and takes place of the Mn^{3+} cations, the decrease of the Curie temperature T_c may be explained by the vanishing of the double exchange between Mn^{3+} and Mn^{4+} ions. The replacement of Mn^{3+} by Bi^{3+} destroys some ratios of Mn^{3+}–O^{2-}–Mn^{4+} bonds and the interactions between Bi–O–Mn might be antiferromagnetic super-exchange. The competition between the Mn–O–Mn double exchange and the Bi–O–Mn super-exchange

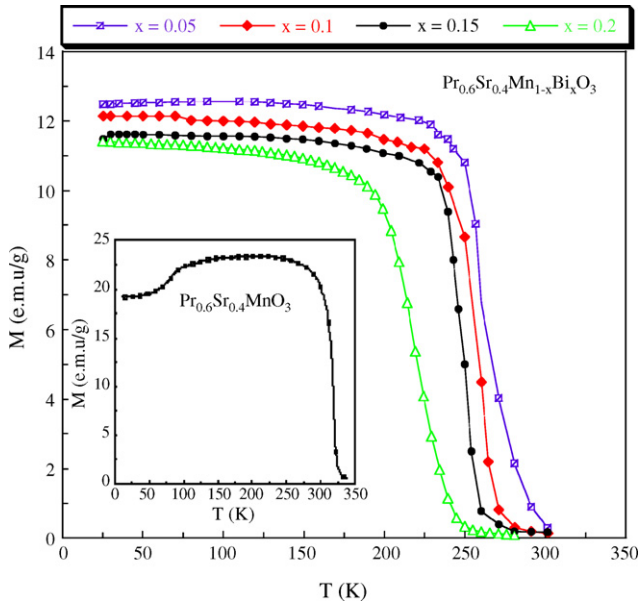

Fig. 4. Evolution of the magnetization as a function of temperature at $H=500$ Oe for $Pr_{0.6}Sr_{0.4}Mn_{1-x}Bi_xO_3$ ($0.0 \le x \le 0.2$).

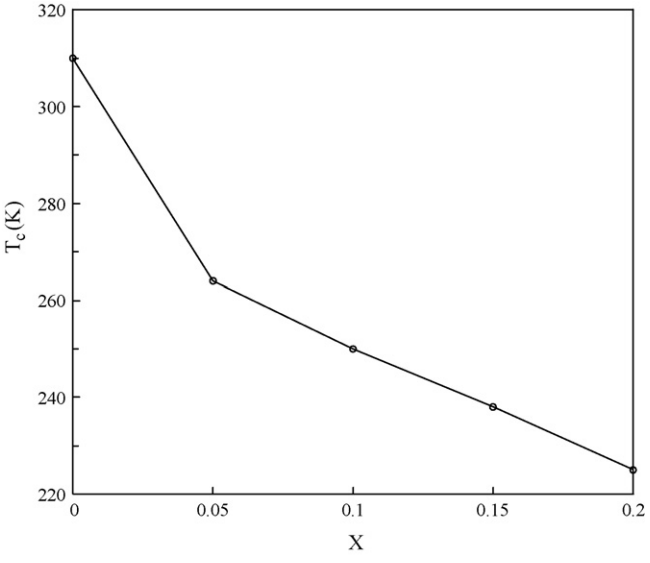

Fig. 5. Curie temperature dependence as a function of x for $Pr_{0.6}Sr_{0.4}Mn_{1-x}Bi_xO_3$ samples.

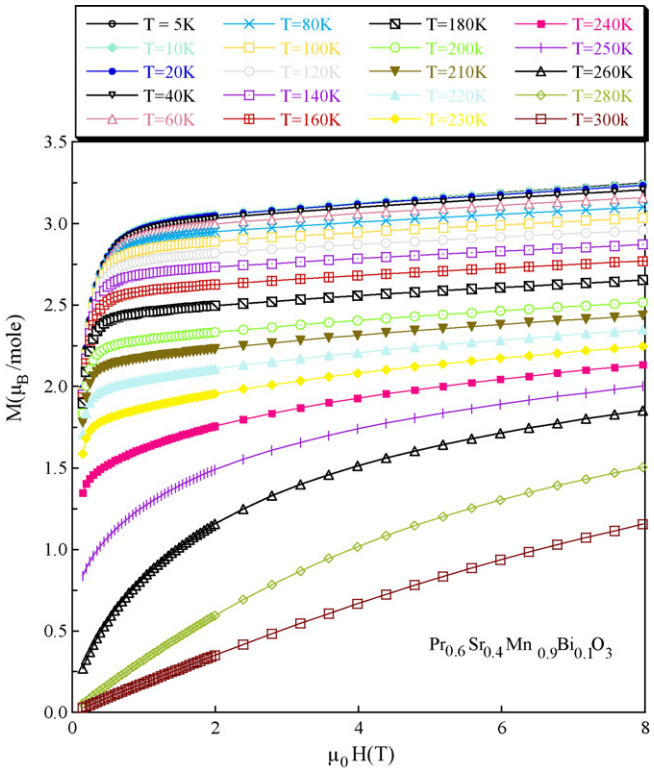

Fig. 6. Magnetization vs. magnetic applied field for several temperatures in $Pr_{0.6}Sr_{0.4}Mn_{0.9}Bi_{0.1}O_3$ sample.

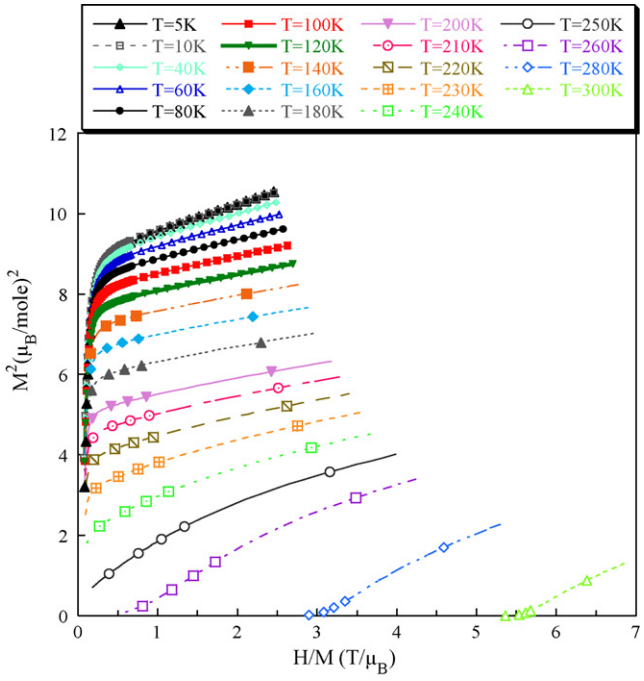

Fig. 7. Arrott curves for $Pr_{0.6}Sr_{0.4}Mn_{0.9}Bi_{0.1}O_3$ sample.

may explain the weakening of the ferromagnetism in our doped samples.

In order to gain a deeper understanding of the magnetic properties and to confirm the ferromagnetic behaviour at low temperatures, we performed field dependent magnetization measurements up to 8 T at several temperatures. We plot in Fig. 6 the $M(H)$ curves for $Pr_{0.6}Sr_{0.4}Mn_{0.9}Bi_{0.1}O_3$. The magnetization, at low temperatures ($T < T_c$), increases sharply with magnetic applied field for $H < 1$ T and then saturates which shows quite typical ferromagnetic behaviour with a saturation magnetization which shifts to higher values with decreasing temperature. In the undoped parent compound $Pr_{0.6}Sr_{0.4}MnO_3$, the magnitude of the saturation magnetization at 10 K is found to be $3.58\mu_B$ which is very close to the theoretical value ($M_{spth} = 3.6\mu_B$) for full alignment of the Mn spin ions. However, it is found to be only $3.05\mu_B$ in the doped $Pr_{0.6}Sr_{0.4}Mn_{0.9}Bi_{0.1}O_3$ sample, whereas the theoretical value of the magnetization for full spin alignment calculated on the basis of 40% of Mn^{4+} and 50% of Mn^{3+} is equal to $3.2\mu_B$. The discrepancy between the theoretical and the experimental values of the saturation magnetization may be explained by the Bi–O–Mn antiferromagnetic super-exchange, it may be also explained by a spin canted state in the Mn^{3+} and Mn^{4+} spins induced by the Bi doping.

In order to determine the Curie temperature with precision, we plot in Fig. 7 the Arrott curves (M^2 versus H/M) for the $Pr_{0.6}Sr_{0.4}Mn_{0.9}Bi_{0.1}O_3$ compound. T_c deduced from these curves is found to be 252 K.

We plot in Fig. 8 the temperature dependence of the spontaneous magnetization (M_{sp}) deduced from the $M(H)$ curves and the inverse of the susceptibility ($1/\chi$) as a function of temperature for $Pr_{0.6}Sr_{0.4}Mn_{0.9}Bi_{0.1}O_3$ sample. The critical exponent γ defined by $M_{sp}(T) = M_{sp}(0)((T_c - T)/T_c)^{\gamma}$ is found to be 0.33 which is in good agreement with the ferromagnetic state.

A large magnetic entropy change was recently observed in perovskite-type ferromagnetic oxides [20,21]. The intense interest in perovskite materials has been prompted by the observation of colossal magnetoresistance effect [22–24]. The magneto-caloric effect can be related to the magnetic properties of the material through the thermodynamic Maxwell's equation $(\partial S/\partial H)_T = (\partial M/\partial T)_H$. From the magnetic properties, the isothermal entropy change of a material can be calculated

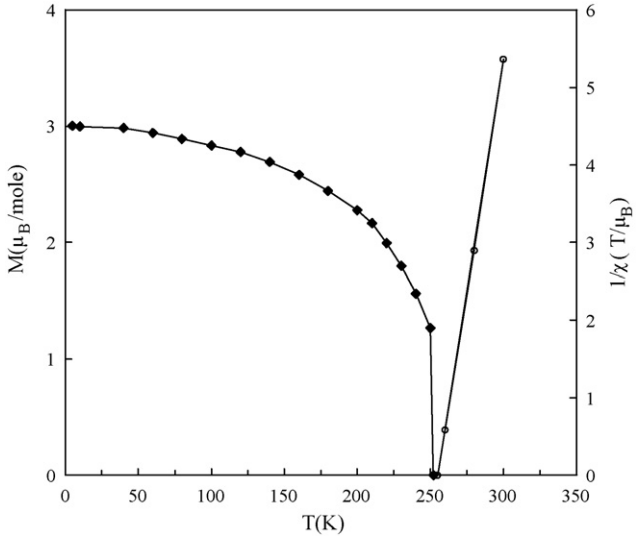

Fig. 8. Spontaneous magnetization and inverse susceptibility vs. temperature for the $Pr_{0.6}Sr_{0.4}Mn_{0.9}Bi_{0.1}O_3$ sample.

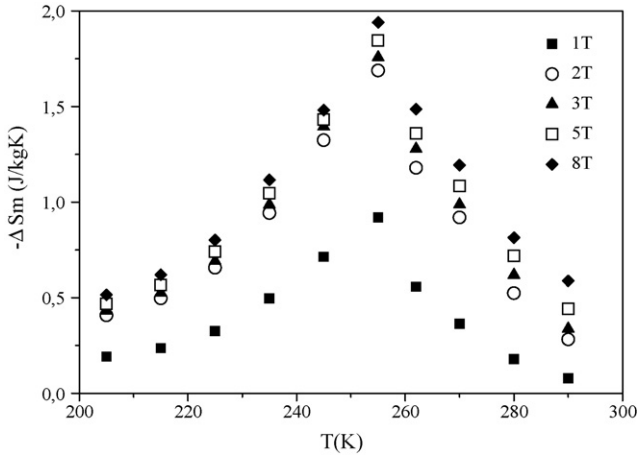

Fig. 9. Temperature dependence of magnetic entropy changes for $Pr_{0.6}Sr_{0.4}Mn_{0.9}Bi_{0.1}O_3$ sample upon several magnetic applied field.

using this relation as $\Delta Sm = \int_0^H (\partial M/\partial T)_H \, dH$. The magnetic entropy change depends on the temperature gradient of the magnetization and reaches its maximum value around the Curie temperature T_c at which the magnetization decays more rapidly. Fig. 9 displays the temperature dependence of the magnetic entropy change of $Pr_{0.6}Sr_{0.4}Mn_{0.9}Bi_{0.1}O_3$ sample upon different magnetic field changes. $|\Delta S_m|$ varies with temperature and reaches its maximum very close to the expected value of 255 K. We can notice that the larger the magnetic field is, the larger the magnetic entropy change is obtained. However, the utmost rise in $|\Delta S_m|$ is obtained when a magnetic field change of 2 T is applied. In fact a maximum of magneto-entropy change of 1.7 J/kg K is achieved whereas it does not exceed 0.95 J/kg K for a magnetic field change of 1 T. Under 8 T, the maximum of $|\Delta S_m|$ does not show a significant improvement and it is about 2 J/kg K.

The large magneto-caloric effect observed mainly in low magnetic field change is high enough to make our samples potential candidates for magnetic refrigeration.

4. Conclusion

$Pr_{0.6}Sr_{0.4}Mn_{1-x}Bi_xO_3$ powder samples have been synthesized using the standard ceramic process for the composition range $0 \leq x \leq 0.2$, we have investigated their structural, magnetic and magneto-caloric properties. The substitution of manganese by bismuth does not induce a great change in the lattice parameters but contributes to a weakening of the ferromagnetic behaviour at low temperature and consequently a decrease in the Curie temperature T_c with increasing Bi content. Our results may be explained by the interruption of the double exchange interaction between Mn^{4+} and Mn^{3+}. The critical exponent γ is found to be $\gamma = 0.33$ for $Pr_{0.6}Sr_{0.4}Mn_{0.9}Bi_{0.1}O_3$ sample. A large magneto-caloric effect is also observed in this sample near 250 K suggesting that this material can be used as magnetic refrigerant.

Acknowledgement

This work has been supported by the Tunisian Ministry of Scientific Research, Technology and Development of Competences.

References

[1] F. Damay, C. Martin, M. Hervieu, A. Maignan, B. Raveau, G. André, F. Bourée, J. Magn. Magn. Mater. 184 (1998) 71.
[2] H.L. Ju, H. Sohn, J. Magn. Magn. Mater. 167 (1997) 200.
[3] Y.H. Huang, C.H. Yan, Z.M. Wang, C.S. Liao, G.X. Xu, Solid State Commun. 118 (2001) 541.
[4] W. Boujelben, A. Cheikh-Rouhou, M. Ellouze, J.C. Joubert, Phys. Stat. Sol. (a) 177 (2000) 503.
[5] A. Peles, H.P. Kunkel, X.Z. Zhou, G. Williams, J. Phys. Condens. Matter 11 (1999) 8111.
[6] W. Boujelben, M. Ellouze, A. Cheikh-Rouhou, J. Pierre, Q. Cai, W.B. Yelon, K. Shimizu, C. Dubourdieu, Phys. Stat. Sol. (a) 191 (2002) 243.
[7] C. Zener, Phys. Rev. 82 (1951) 403.
[8] A.J. Millis, P.B. Littlewood, B.I. Shraiman, Phys. Rev. Lett. 74 (1955) 5144.
[9] F. Damay, C. Martin, A. Martin, B. Raveau, J. Appl. Phys. 81 (1997) 1372.
[10] L.M. Rodriguez-Martinez, J.P. Atfield, Phys. Rev. B 54 (1996) 15622.
[11] I.O. Troyanchuk, S.V. Trukanov, H. Szymezak, K. Baerner, J. Phys. Condens. Matter 12 (2000) L155.
[12] S. Jin, M. McCormack, T.H. Tiefel, R. Ramesh, J. Appl. Phys. 76 (1994) 6929.
[13] W. Boujelben, M. Ellouze, A. Cheikh-Rouhou, J. Pierre, Q. Cai, W.B. Yelon, K. Shimizu, C. Dubourdieu, J. Alloys Compd. 334 (2002) 1.
[14] W. Boujelben, M. Ellouze, A. Cheikh-Rouhou, H. Fuess, Phys. Stat. Sol. (a) 189 (2002) 837.
[15] W. Boujelben, A. Cheikh-Rouhou, M. Ellouze, R. Madar, H. Fuess, Phys. Stat. Sol. (a) 201 (2004) 1410.
[16] A. Ammar, S. Zouari, A. Cheikh-Rouhou, Phys. Stat. Sol. (c) 1 (2004) 1645.
[17] A. Ammar, S. Zouari, A. Cheikhrouhou, J. Alloys Compd. 354 (2003) 85.
[18] Y. Li, J. Miao, Y. Sui, Z. Lü, Z. Qian, W. Su, J. Magn. Magn. Mater. 305 (2006) 247.
[19] D.B. Wiles, R.A. Young, J. Appl. Crystallogr. 14 (1981) 149.
[20] Z.B. Guo, Y.W. Du, D. Feng, Phys. Rev. Lett. 78 (1997) 1142.
[21] Z.B. Guo, Y.W. Du, Appl. Phys. Lett. 70 (1997) 904.
[22] P. Schiffer, Z.A.P. Ramirez, S.W. Cheng, Phys. Rev. Lett. 75 (1995) 3336.
[23] H.L. Ju, C. Kwong, T. Venkatesan, Appl. Phys. Lett. 65 (1994) 2108.
[24] J. Barratt, M.R. Lees, D. Mck-Paul, Appl. Phys. Lett. 68 (1996) 424.